TECHNICAL ARTICLE

Crystal structure of rivastigmine hydrogen tartrate Form I (Exelon®), $C_{14}H_{23}N_2O_2(C_4H_5O_6)$

James A. Kaduk,[1,a] Kai Zhong,[2] Amy M. Gindhart,[2] and Thomas N. Blanton[2]
[1]*Illinois Institute of Technology, 3101 S. Dearborn St., Chicago Illinois 60616*
[2]*ICDD, 12 Campus Blvd., Newtown Square, Pennsylvania, 19073-3273*

(Received 14 June 2015; accepted 20 January 2016)

The crystal structure of rivastigmine hydrogen tartrate has been solved and refined using synchrotron X-ray powder diffraction data, and optimized using density functional techniques. Rivastigmine hydrogen tartrate crystallizes in space group $P2_1$ (#4) with $a = 17.538\ 34(5)$, $b = 8.326\ 89(2)$, $c = 7.261\ 11(2)$ Å, $\beta = 98.7999(2)°$, $V = 1047.929(4)$ Å^3, and $Z = 2$. The un-ionized end of the hydrogen tartrate anions forms a very strong hydrogen bond with the ionized end of another anion to form a chain. The ammonium group of the rivastigmine cation forms a strong discrete hydrogen bond with the carbonyl oxygen atom of the un-ionized end of the tartrate anion. These hydrogen bonds form a corrugated network in the *bc*-plane. Both hydroxyl groups of the tartrate anion form intramolecular O–H···O hydrogen bonds. Several C–H···O hydrogen bonds appear to contribute to the crystal energy. The powder pattern is included in the Powder Diffraction File™ as entry 00-064-1501. © *2016 International Centre for Diffraction Data*. [doi:10.1017/S0885715616000038]

Key words: rivastigmine hydrogen tartrate, Exelon, powder diffraction, Rietveld refinement, density functional theory

I. INTRODUCTION

Rivastigmine hydrogen tartrate (Exelon®), also called rivastigmine tartrate, is a cholinergic agent used to treat Alzheimer's disease and Parkinson's disease. The systematic name (CAS Registry number 129101-54-8) is (*S*)-*N*-ethyl-*N*-methyl-3-[1-(dimethylamino)-ethyl]-phenyl carbamate hydrogen-(*2R,3R*)-tartrate. A two-dimensional molecular diagram is shown in Figure 1. Crystalline Forms I and II (as well as amorphous) of rivastigmine hydrogen tartrate are claimed in European Patent Application 1942100 (Benkic *et al.*, 2008), and crystalline Form II is also claimed in US Patent Application 2008/0255231 (Overeem and Vinent, 2008).

The presence of high-quality reference powder patterns in the Powder Diffraction File (PDF; ICDD, 2014) is important for phase identification, particularly by pharmaceutical, forensic, and law enforcement scientists. The crystal structures of a significant fraction of the largest dollar volume pharmaceuticals have not been published, and thus calculated powder patterns are not present in the PDF-4 databases. Sometimes experimental patterns are reported, but they are generally of low quality. This structure is a result of the collaboration among International Centre for Diffraction Data (ICDD), Illinois Institute of Technology (IIT), Poly Crystallography Inc., and Argonne National Laboratory to measure high-quality synchrotron powder patterns of commercial pharmaceutical ingredients, include these reference patterns in the PDF, and determine the crystal structures of these Active Pharmaceutical Ingredients (APIs).

Even when the crystal structure of an API is reported, the single crystal structure was often determined at low temperature. Most powder measurements are performed at ambient conditions. Thermal expansion (generally anisotropic) means that the peak positions calculated from a low-temperature single crystal structure often differ significantly from those measured at ambient conditions. These peak shifts can result in a failure of default search/match algorithms to identify a phase, even when it is present in the sample. High-quality reference patterns measured at ambient conditions are thus critical for easy identification of APIs using standard powder diffraction practices.

II. EXPERIMENTAL

"Rivastigmine tartrate" was a commercial reagent, purchased from Tocris Bioscience (Batch No. 1A/129729), and was used as-received. The white powder was packed into a 1.5 mm diameter Kapton capillary, and rotated during the measurement at ~50 cycles s^{-1}. The powder pattern was measured at 295 K at beam line 11-BM (Lee *et al.*, 2008; Wang *et al.*, 2008) of the Advanced Photon Source at Argonne National Laboratory using a wavelength of 0.413 891 Å from 0.5° to 50° 2θ with a step size of 0.001° and a counting

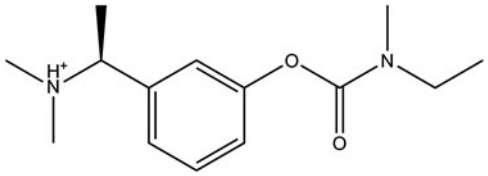

Figure 1. The molecular structure of the rivastigmine cation.

a)Author to whom correspondence should be addressed. Electronic mail: kaduk@polycrystallography.com

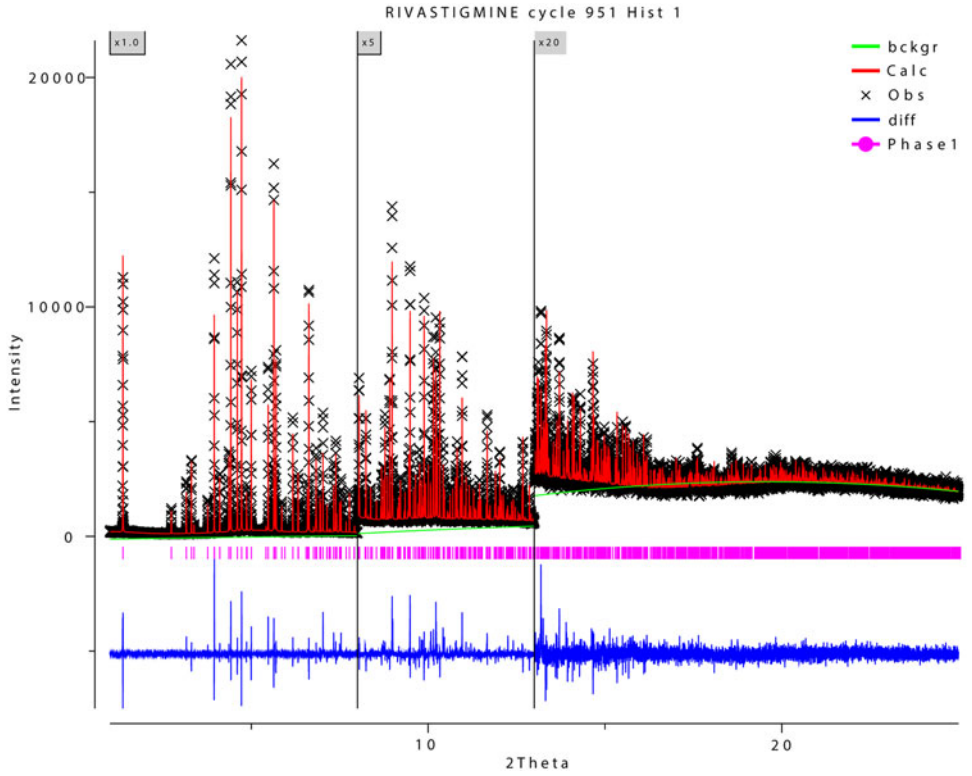

Figure 2. (Color online) The Rietveld plot for the refinement of rivastigmine hydrogen tartrate Form I. The black crosses represent the observed data points, and the red line is the calculated pattern. The blue curve is the difference pattern, plotted at the same vertical scale as the other patterns, and the green line is the background. The vertical scale has been multiplied by a factor of 5 for $2\theta > 8.0°$, and by a factor of 20 for $2\theta > 13.0°$.

time of 0.1 s step^{-1}. The pattern was indexed on a primitive monoclinic unit cell having $a = 17.509$, $b = 8.358$, $c = 7.299$ Å, $\beta = 98.866°$, $V = 2190$ Å^3, and $Z = 2$ using Jade 9.5 (MDI, 2014) and N-TREOR in EXPO2009 (Altomare *et al.*, 2009). Analysis of the systematic absences in EXPO2009 suggested the space group $P2_1$, which was confirmed by successful solution and refinement of the structure. A reduced cell search in the Cambridge Structural Database (Allen, 2002) combined with chemistry "C H N O only" yielded 34 hits, but no structure for rivastigmine hydrogen tartrate. A name search on "rivastigmine" yielded (*S*)-rivastigmine (+)di (*p*-toluoyl)-D-tartaric acid (Chen *et al.*, 2009; CSD Refcode MAKKEQ), as did a connectivity search on rivastigmine.

A rivastigmine dication and a tartrate dianion were built and their conformations optimized using Spartan '14 (Wavefunction, 2013), and saved as mol2 files. These files were converted into Fenske–Hall *Z*-matrix files using OpenBabel (O'Boyle *et al.*, 2011). Using these two fragments, the structure was solved with DASH (David *et al.*, 2006). In the best solution, it was clear that N20 participated in a strong hydrogen bond, but that N14 did not. In addition, the tartrate oxygen atoms O48 and O51 were close (~2.50 Å), suggesting that they formed a very strong hydrogen bond, and that a hydrogen atom was present between them. The compound is thus not rivastigmine tartrate, but rivastigmine hydrogen tartrate, as expected from the patent literature.

Rietveld refinement was carried out using GSAS (Toby, 2001; Larson and Von Dreele, 2004). Only the 1.0°–25.0° portion of the pattern was included in the refinement ($d_{min} = 0.955$ Å).

The C1–H10 benzene ring was refined as a rigid body. The *y*-coordinate of O11 was fixed to determine the origin. All non-H bond distances and angles were subjected to restraints, based on a Mercury/Mogul Geometry Check (Bruno *et al.*, 2004; Sykes *et al.*, 2011) of the molecule. The Mogul average and standard deviation for each quantity were used as the restraint parameters. The restraints contributed 6.78% to the final χ^2. Isotropic displacement coefficients were refined, grouped by chemical similarity. The hydrogen atoms were included in calculated positions, which were recalculated using Materials Studio during the refinement. The U_{iso} of each hydrogen atom was constrained to be 1.3× that of the heavy atom to which it is attached. Initial positions of the active hydrogens were deduced from an analysis of potential hydrogen bonding patterns. The peak profiles were described using profile function #4 (Thompson *et al.*, 1987; Finger *et al.*, 1994), which includes the Stephens (1999) anisotropic strain broadening model. The background was modeled using a three-term shifted Chebyshev polynomial, with a 15-term diffuse scattering function to model the Kapton capillary and any amorphous component. The final refinement (started from the result of the density functional theory (DFT) calculation) of 95 variables using 24 050 observations (23 999 data points and 51 restraints) yielded the residuals $R_{wp} = 0.1091$, $R_p = 0.0915$, and $\chi^2 = 2.405$. The largest peak (0.21 Å from N14) and hole (0.76 Å from C12) in the difference Fourier map were 0.62 and -0.50 eÅ^{-3}, respectively. The Rietveld plot is included as Figure 2. The largest errors are in the shapes and positions of the low-angle peaks, and may indicate subtle changes in the sample during the measurement.

A density functional geometry optimization (fixed experimental unit cell) was carried out using CRYSTAL09 (Dovesi *et al.*, 2005). The basis sets for the H, C, N, and O atoms were those of Gatti *et al.* (1994). The calculation used 8 *k*-points and the B3LYP functional, and took ~13 days on a 2.4 GHz PC.

https://doi.org/10.1017/S0885715616000038 Published online by Cambridge University Press

TABLE I. Rietveld refined crystal structure of rivastigmine hydrogen tartrate.

Crystal data	
$C_{14}H_{23}N_2O_2(C_4H_5O_6)$	$\beta = 98.7999\ (2)^\circ$
$M_r = 200.21$	$V = 1047.93\ (1)$ Å^3
Monoclinic, $P2_1$	$Z = 2$
$a = 17.538\ 34\ (5)$ Å	Synchrotron radiation, $\lambda = 0.413\ 891$ Å
$b = 8.326\ 893\ (18)$ Å	$T = 293$ K
$c = 7.261\ 113\ (15)$ Å	Cylinder, 1.5×1.5 mm^2

Data collection	
11-BM APS diffractometer	Scan method: step
Specimen mounting: Kapton capillary	$2\theta_{min} = 0.5^\circ$, $2\theta_{max} = 50.0^\circ$, $2\theta_{step} = 0.001^\circ$
Data collection mode: transmission	

Refinement	
Least-squares matrix: full	49 495 data points
$R_p = 0.092$	Profile function: CW Profile function number 4 with 21 terms Pseudovoigt profile coefficients as parameterized in Thompson *et al.* (1987). Asymmetry correction of Finger *et al.* (1994). Microstrain broadening by Stephens (1999). #1(GU) = 1.163 #2 (GV) = −0.126 #3(GW) = 0.063 #4(GP) = 0.000 #5(LX) = 0.173 #6(ptec) = 0.00 #7 (trns) = 0.00 #8(shft) = 0.0000 #9(sfec) = 0.00 #10(S/L) = 0.0011 #11(H/L) = 0.0011 #12(eta) = 1.0000 #13(S400) = 1.2×10^{-5} #14(S040) = 4.5×10^{-4} #15(S004) = 3.1×10^{-5} #16(S220) = -7.6×10^{-5} #17(S202) = -1.0×10^{-5} #18(S022) = -4.4×10^{-5} #19(S301) = 3.6E-06 #20(S103) = -2.9×10^{-5} #21(S121) = 3.7×10^{-5} Peak tails are ignored where the intensity is below 0.0010 times the peak Aniso. broadening axis 0.0 0.0 1.0
$R_{wp} = 0.109$	100 parameters
$R_{exp} = 0.073$	51 restraints
$R(F^2) = 0.170\ 47$	$(\Delta/\sigma)_{max} = 0.02$
$\chi^2 = 2.403$	Background function: GSAS Background function number 1 with 3 terms. Shifted Chebyshev function of 1st kind 1: 37.1375 2: 112.196 3: −51.2900

Fractional atomic coordinates and isotropic displacement parameters (Å^2)

	x	y	z	U_{iso}*/U_{eq}
C1	0.3415 (3)	0.6074 (6)	0.3321 (7)	0.0695 (17)*
C2	0.2899 (3)	0.6353 (7)	0.4564 (7)	0.0695 (17)*
C3	0.2638 (2)	0.5078 (8)	0.5539 (6)	0.0695 (17)*
C4	0.2893 (3)	0.3525 (7)	0.5273 (7)	0.0695 (17)*
C5	0.3409 (3)	0.3246 (6)	0.4031 (7)	0.0695 (17)*
C6	0.3671 (2)	0.4520 (7)	0.3055 (6)	0.0695 (17)*
H7	0.2690 (4)	0.7625 (7)	0.4783 (10)	0.090 (2)*
H8	0.2679 (4)	0.2481 (8)	0.6072 (10)	0.090 (2)*
H9	0.3618 (4)	0.1974 (6)	0.3813 (10)	0.090 (2)*
H10	0.4093 (3)	0.4291 (8)	0.2038 (8)	0.090 (2)*
O11	0.3471 (3)	0.724 47	0.1911 (7)	0.218 (3)*
C12	0.4151 (4)	0.8004 (11)	0.2147 (10)	0.218 (3)*
O13	0.4578 (5)	0.7574 (11)	0.3533 (11)	0.218 (3)*
N14	0.4254 (5)	0.9285 (13)	0.1415 (12)	0.218 (3)*
C15	0.3735 (6)	1.0030 (15)	−0.0139 (16)	0.218 (3)*
C16	0.3999 (8)	0.947 (2)	−0.1774 (16)	0.218 (3)*
C17	0.5060 (6)	0.9870 (19)	0.1874 (18)	0.218 (3)*
C18	0.1995 (2)	0.5354 (9)	0.6682 (6)	0.0764 (17)*
C19	0.2155 (4)	0.4573 (12)	0.8629 (8)	0.0764 (17)*
N20	0.1230 (2)	0.4778 (10)	0.5662 (7)	0.0764 (17)*
C21	0.0634 (3)	0.4625 (12)	0.6902 (9)	0.0764 (17)*
C22	0.0940 (4)	0.5741 (12)	0.3959 (9)	0.0764 (17)*
H23	0.189 76	0.997 81	0.582 06	0.080 (4)*
H24	0.378 33	1.139 41	−0.005 28	0.283 (4)*
H25	0.311 58	0.963 98	−0.008 43	0.283 (4)*
H26	0.370 54	1.017 12	−0.303 05	0.283 (4)*
H27	0.385 32	0.813 62	−0.197 48	0.283 (4)*
H28	0.465 05	0.963 37	−0.163 03	0.283 (4)*
H29	0.526 65	1.032 07	0.055 21	0.283 (4)*
H30	0.544 76	0.884 61	0.2497	0.283 (4)*
H31	0.5085	1.089 26	0.292 54	0.283 (4)*
H32	0.194 62	0.670 47	0.689 22	0.099 (2)*

Continued

https://doi.org/10.1017/S0885715616000038 Published online by Cambridge University Press

TABLE I. Continued

	x	y	z	U_{iso}*/U_{eq}
H33	0.270 47	0.510 29	0.944 38	0.099 (2)*
H34	0.222 88	0.322 19	0.847 44	0.099 (2)*
H35	0.164 98	0.481 69	0.940 78	0.099 (2)*
H36	0.133 36	0.351 28	0.5154	0.099 (2)*
H37	0.081 54	0.535 51	0.822 46	0.099 (2)*
H38	0.005 88	0.509 38	0.615	0.099 (2)*
H39	0.057 05	0.330 87	0.728 29	0.099 (2)*
H40	0.056 08	0.4952	0.290 95	0.099 (2)*
H41	0.145 03	0.620 36	0.331 09	0.099 (2)*
H42	0.0588	0.680 12	0.435 89	0.099 (2)*
C43	0.1540 (4)	1.0866 (10)	0.3633 (5)	0.0567 (7)*
C44	0.1507 (2)	1.0927 (9)	0.1517 (5)	0.0567 (7)*
C45	0.1404 (3)	0.9234 (9)	0.0679 (5)	0.0567 (7)*
C46	0.1347 (3)	0.9309 (11)	−0.1459 (5)	0.0567 (7)*
O47	0.1059 (3)	1.1714 (10)	0.4283 (6)	0.0567 (7)*
O48	0.1968 (3)	0.9829 (9)	0.4511 (6)	0.0567 (7)*
O49	0.0884 (3)	1.1927 (8)	0.0789 (6)	0.0567 (7)*
O50	0.0742 (3)	0.8481 (9)	0.1201 (6)	0.0567 (7)*
O51	0.1905 (3)	0.9909 (10)	−0.2074 (6)	0.0567 (7)*
O52	0.0764 (3)	0.8713 (11)	−0.2424 (6)	0.0567 (7)*
H53	0.2066	1.146 55	0.1177	0.0771 (9)*
H54	0.193 28	0.849	0.125 37	0.0771 (9)*
H55	0.037 62	1.169 65	0.004 38	0.0771 (9)*
H56	0.045 47	0.864 54	−0.008 63	0.0771 (9)*

TABLE II. DFT-optimized (CRYSTAL09) crystal structure of rivastigmine hydrogen tartrate.

Crystal data	
$C_{14}H_{23}N_2O_2(C_4H_5O_6)$	$\beta = 98.7999°$
$M_w = 400.20$	$V = 1047.93$ Å^3
Monoclinic, $P2_1$	$Z = 2$
$a = 17.5384$ Å	
$b = 8.3269$ Å	
$c = 7.2611$ Å	

Fractional atomic coordinates and isotropic displacement parameters (Å^2)

	x	y	Z	U_{iso}
C1	0.340 43	0.598 34	0.290 97	0.079 20
C2	0.285 27	0.627 26	0.406 01	0.079 20
C3	0.259 46	0.500 76	0.507 75	0.079 20
C4	0.290 48	0.347 00	0.492 48	0.079 20
C5	0.346 36	0.320 36	0.378 22	0.079 20
C6	0.371 81	0.446 22	0.276 40	0.079 20
H7	0.262 58	0.747 96	0.413 56	0.103 00
H8	0.271 78	0.247 08	0.570 07	0.103 00
H9	0.371 41	0.201 78	0.371 88	0.103 00
H10	0.415 85	0.427 95	0.188 83	0.103 00
O11	0.360 68	0.724 47	0.182 20	0.215 10
C12	0.428 80	0.804 39	0.246 91	0.215 10
O13	0.473 86	0.758 26	0.381 67	0.215 10
N14	0.438 58	0.934 22	0.140 42	0.215 10
C15	0.379 89	0.994 62	−0.010 22	0.215 10
C16	0.399 56	0.968 31	−0.206 26	0.215 10
C17	0.508 88	1.028 68	0.193 83	0.215 10
C18	0.200 83	0.533 17	0.637 83	0.080 90
C19	0.219 50	0.441 52	0.821 94	0.080 90
N20	0.118 63	0.495 58	0.540 94	0.080 90
C21	0.059 67	0.498 42	0.671 04	0.080 90
C22	0.093 84	0.604 94	0.378 35	0.080 90
H23	0.191 89	0.993 75	−0.454 56	0.077 20
H24	0.372 20	1.123 21	0.014 71	0.279 60
H25	0.325 29	0.936 02	0.000 05	0.279 60
H26	0.349 12	1.000 22	−0.307 66	0.279 60
H27	0.412 45	0.842 02	−0.229 02	0.279 60
H28	0.447 88	1.041 78	−0.236 17	0.279 60
H29	0.523 50	1.088 76	0.070 19	0.279 60
H30	0.556 11	0.949 33	0.250 90	0.279 60
H31	0.501 90	1.118 35	0.300 49	0.279 60
H32	0.199 90	0.662 13	0.665 76	0.105 20
H33	0.279 73	0.463 98	0.880 15	0.105 20
H34	0.211 46	0.312 14	0.802 06	0.105 20
H35	0.183 61	0.479 70	0.923 97	0.105 20
H36	0.117 78	0.379 97	0.486 97	0.105 20
H37	0.070 58	0.399 52	0.769 39	0.105 20
H38	0.003 17	0.486 13	0.586 52	0.105 20
H39	0.063 40	0.614 33	0.741 39	0.105 20
H40	0.035 07	0.571 74	0.320 07	0.105 20
H41	0.132 07	0.587 45	0.275 36	0.105 20
H42	0.095 78	0.728 30	0.428 56	0.105 20
C43	0.146 85	1.098 72	0.308 59	0.059 40
C44	0.146 87	1.100 22	0.096 92	0.059 40
C45	0.130 96	0.933 62	0.007 60	0.059 40
C46	0.133 47	0.941 44	−0.204 43	0.059 40
O47	0.106 61	1.192 68	0.382 08	0.059 40
O48	0.193 67	0.992 79	0.399 08	0.059 40
O49	0.093 86	1.214 91	0.009 84	0.059 40
O50	0.056 75	0.879 59	0.035 83	0.059 40
O51	0.196 80	0.983 93	−0.255 37	0.059 40
O52	0.072 63	0.901 39	−0.307 86	0.059 40
H53	0.204 46	1.138 12	0.073 92	0.080 50
H54	0.175 36	0.849 67	0.072 03	0.080 50
H55	0.042 65	1.171 90	0.011 63	0.080 50
H56	0.027 46	0.875 47	−0.090 41	0.080 50

https://doi.org/10.1017/S0885715616000038 Published online by Cambridge University Press

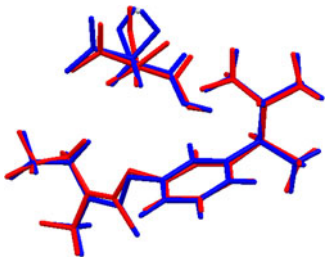

Figure 3. (Color online) Comparison of the refined and optimized structures of rivastigmine hydrogen tartrate. The Rietveld refined structure is in red, and the DFT-optimized structure is in blue.

III. RESULTS AND DISCUSSION

The experimental pattern corresponds to that of Form I reported by Benkic *et al.* (2008). The refined atom coordinates of rivastigmine hydrogen tartrate are reported in Table I, and the coordinates from the DFT optimization in Table II. The root-mean-square (rms) deviation of the non-hydrogen atoms in the rivastigmine is 0.206 Å (Figure 3), and the rms deviation in the tartrate is 0.091 Å. The largest difference (0.360 Å) is at the methyl group C17. This good agreement between the refined and optimized structures is evidence that the experimental structure is correct (van de Streek and Neumann, 2014). This discussion uses the DFT-optimized structure. The asymmetric unit (with atom numbering) is illustrated in Figure 4, and the crystal structure is presented in Figure 5.

All of the bond distances, bond angles and torsion angles fall within the normal ranges indicated by a Mercury Mogul Geometry check (Macrae *et al.*, 2008). The displacement coefficients of the methylethylamino group N14–C17 are large, perhaps indicating that this group is disordered. There is no obvious sign of disorder in the difference Fourier map, and since the refined structure was to be used as input to an (ordered) DFT calculation, any disorder was not pursued further.

A quantum mechanical conformation examination (Hartree-Fock/6-21G*/water) using Spartan '14 indicated that the observed conformation of the rivastigmine cation is ~6.9 kcal mole^{-1} higher in energy than a local minimum. A

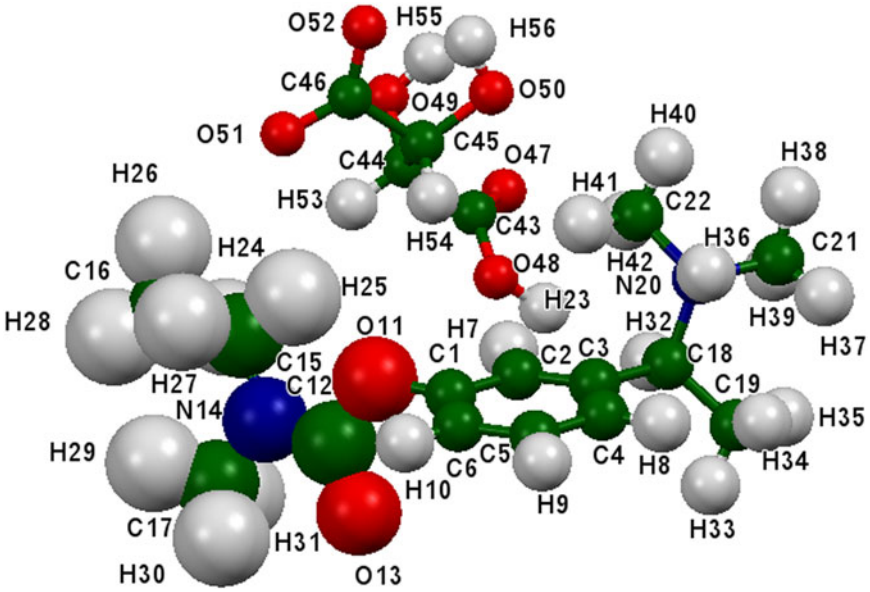

Figure 4. (Color online) The molecular structure of rivastigmine hydrogen tartrate, with the atom numbering. The atoms are represented by 50% probability spheroids.

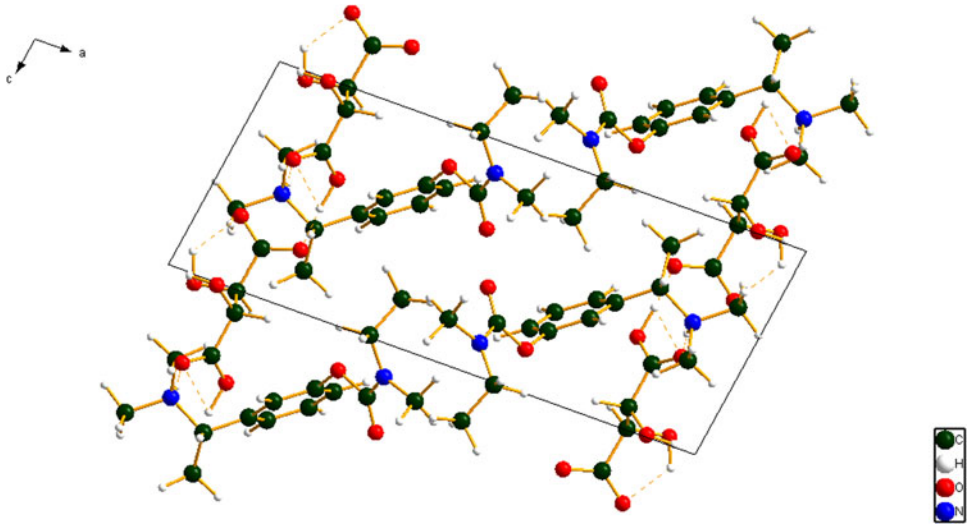

Figure 5. (Color online) The crystal structure of rivastigmine hydrogen tartrate, viewed down the *b*-axis. The hydrogen bonds are shown as dashed lines.

https://doi.org/10.1017/S0885715616000038 Published online by Cambridge University Press

TABLE III. Hydrogen bonds in the DFT-optimized crystal structure of rivastigmine hydrogen tartrate.

D–H···A	D–H (Å)	H···A (Å)	D···A (Å)	D–H···A (°)	Overlap (*e*)
O48–H23···O51	1.068	1.438	2.502	173.8	0.101
O50–H56···O52	0.980	1.884	2.559	123.5	0.054
O49–H55···O50	0.969	2.442	2.950	112.3	0.012
N20–H36···O47	1.039	1.733	2.768	173.6	0.069
C2–H7···O48	1.085	2.364	3.438	170.1	0.022
C15–H25···O11	1.087	2.233	2.696	103.1	0.010
C17–H30···O13	1.092	2.436	2.750	94.8	0.009

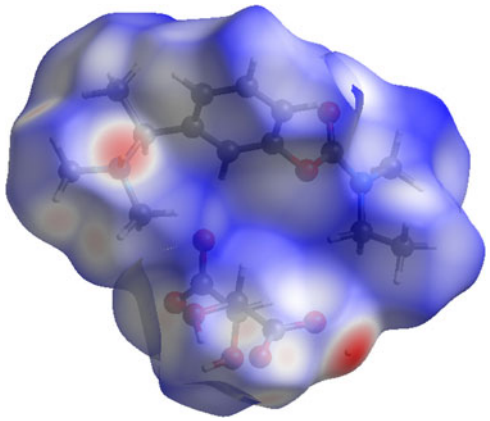

Figure 6. (Color online) The Hirshfeld surface of rivastigmine hydrogen tartrate. Intermolecular contacts longer than the sums of the van der Waals radii are colored blue, and contacts shorter than the sums of the radii are colored red. Contacts equal to the sums of radii are white.

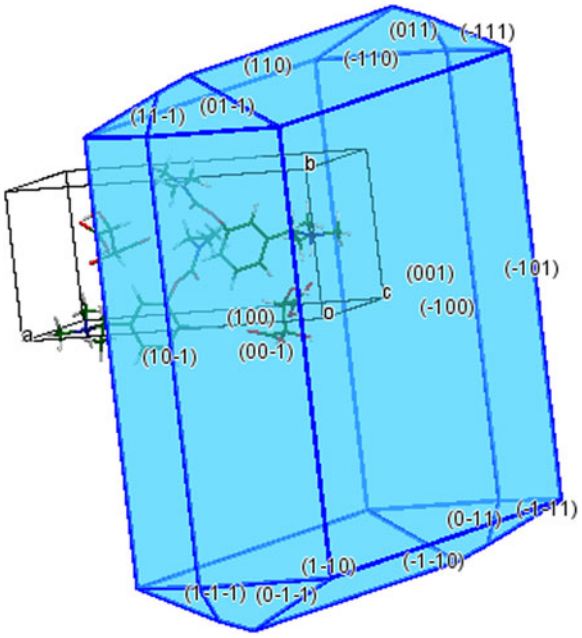

Figure 7. (Color online) The Bravais–Friedel–Donnay–Harker morphology of rivastigmine hydrogen tartrate Form I. The morphology is platy, with {100} as the major faces.

molecular mechanics (MMFF) sampling of conformational space indicated that the solid state conformation is within 1.2 kcal mole^{-1} of the minimum energy conformation, which is very different than the observed one. The rivastigmine cation appears to be flexible, and has distorted to accommodate the formation of hydrogen bonds. Compared with MAKKEQ (Chen *et al.*, 2009), both methylethylamine ends of the molecule have different conformations.

Analysis of the contributions to the total crystal energy using the Forcite module of Materials Studio (Accelrys, 2013) suggests that the intramolecular deformation energy contains small contributions from bond and angle distortion terms. The intermolecular energy is dominated by electrostatic contributions, which in this force-field-based analysis includes hydrogen bonds. The hydrogen bonds are better analyzed using the results of the DFT calculation.

The un-ionized end of the hydrogen tartrate anions forms a very strong (17.4 kcal mole^{-1}) O48–H23···O51 hydrogen bond with the ionized end of another anion to form a chain (Table III). The graph set is *C1,1(7)* (Etter, 1990; Bernstein *et al.*, 1995; Shields *et al.*, 2000). The ammonium ion N20–H36 forms a strong discrete (graph set *D1,1(2)*) hydrogen bond with the carbonyl oxygen O47 of the un-ionized end of the tartrate anion. Both of these strong hydrogen bonds participate in a discrete pattern with graph set *D3,3(12)*. These hydrogen bonds form a corrugated network in the *bc*-plane. Both hydroxyl groups of the tartrate anion form intramolecular O–H···O hydrogen bonds. Several C–H···O hydrogen bonds appear to contribute to the crystal energy.

The volume enclosed by the Hirshfeld surface (Figure 6; Hirshfeld, 1977; McKinnon *et al.*, 2004; Spackman and Jayatilaka, 2009; Wolff *et al.*, 2012) is 516.62 Å^3, 98.6% of half the unit cell volume. The molecules are thus not tightly packed. The only significant close contacts (red in Figure 6) involve the hydrogen bonds.

The Bravais–Friedel–Donnay–Harker (Bravais, 1866; Friedel, 1907; Donnay and Harker, 1937) morphology suggests that we might expect platy morphology for rivastigmine hydrogen tartrate, with {100} as the principal faces (Figure 7). A second-order spherical harmonic preferred orientation model was included in the refinement; the texture index was 1.016, indicating that preferred orientation was not significant in this rotated capillary specimen. The powder pattern of rivastigmine hydrogen tartrate has been submitted to ICDD for inclusion in the PDF as entry 00-064-1501.

ACKNOWLEDGEMENTS

The use of the Advanced Photon Source at Argonne National Laboratory was supported by the U. S. Department of Energy, Office of Science, Office of Basic Energy Sciences, under Contract No. DE-AC02-06CH11357. This work was partially supported by the International Centre for

Diffraction Data. We thank Lynn Ribaud for his assistance in data collection.

SUPPLEMENTARY MATERIAL

To view supplementary material for this article, please visit http://dx.doi.org/10.1017/S0885715616000038

Accelrys (**2013**). *Materials Studio 7.0* (Accelrys Software Inc., San Diego, CA).

Allen, F. H. (**2002**). "The Cambridge Structural Database: a quarter of a million crystal structures and rising," Acta Crystallogr., B: Struct. Sci. **58**, 380–388.

Altomare, A., Camalli, M., Cuocci, C., Giacovazzo, C., Moliterni, A., and Rizzi, R. (**2009**). "EXPO2009: structure solution by powder data in direct and reciprocal space," J. Appl. Crystallogr. **42**(6), 1197–1202.

Benkic, P., Smrkolj, M., Pecavar, A., Stropnik, T., Vrbinc, M., Vrecer, F., and Pelko, M. (**2008**). "Amorphous and crystalline forms of rivastigmine hydrogen tartrate," European Patent Application 1942100.

Bernstein, J., Davis, R. E., Shimoni, L., and Chang, N. L. (**1995**). "Patterns in hydrogen bonding: functionality and graph set analysis in crystals," Angew. Chem. Int. Ed. Engl. **34**(15), 1555–1573.

Bravais, A. (**1866**). *Etudes Cristallographiques* (Gauthier Villars, Paris).

Bruno, I. J., Cole, J. C., Kessler, M., Luo, J., Motherwell, W. D. S., Purkis, L. H., Smith, B. R., Taylor, R., Cooper, R. I., Harris, S. E., and Orpen, A. G. (**2004**). "Retrieval of crystallographically-derived molecular geometry information," J. Chem. Inf. Sci. **44**, 2133–2144.

Chen, W. M., Wen, F. H., Jin, F., and Mi, J. (**2009**). "Synthesis and crystal structure of *(S)*-rivastigmine D-(+)-DTTA," Huaxue Shiji (Chin.) (Chemical Reagents) 7, 010; CSD Refcode MAKKEQ.

David, W. I. F., Shankland, K., van de Streek, J., Pidcock, E., Motherwell, W. D. S., and Cole, J. C. (**2006**). "DASH: a program for crystal structure determination from powder diffraction data," J. Appl. Crystallogr. **39**, 910–915.

Donnay, J. D. H. and Harker, D. (**1937**). "A new law of crystal morphology extending the law of Bravais," Am. Mineral. **22**, 446–467.

Dovesi, R., Orlando, R., Civalleri, B., Roetti, C., Saunders, V. R., and Zicovich-Wilson, C. M. (**2005**). "CRYSTAL: a computational tool for the *ab initio* study of the electronic properties of crystals," Zeit. Krist. **220**, 571–573.

Etter, M. C. (**1990**). "Encoding and decoding hydrogen-bond patterns of organic compounds," Acc. Chem. Res. **23**(4), 120–126.

Finger, L. W., Cox, D. E., and Jephcoat, A. P. (**1994**). "A correction for powder diffraction peak asymmetry due to axial divergence," J. Appl. Crystallogr. **27**(6), 892–900.

Friedel, G. (**1907**). "Etudes sur la loi de Bravais," Bull. Soc. Fr. Mineral. **30**, 326–455.

Gatti, C., Saunders, V. R., and Roetti, C. (**1994**). "Crystal-field effects on the topological properties of the electron-density in molecular crystals – the case of urea," J. Chem. Phys. **101**, 10686–10696.

Hirshfeld, F. L. (**1977**). "Bonded-atom fragments for describing molecular charge densities," Theor. Chem. Acta **44**, 129–138.

ICDD (**2014**). PDF-4+ 2014 (Database), edited by Dr. Soorya Kabekkodu, International Centre for Diffraction Data, Newtown Square, PA, USA.

Larson, A. C. and Von Dreele, R. B. (**2004**). *General Structure Analysis System (GSAS)* (Report LAUR 86-784). Los Alamos, New Mexico: Los Alamos National Laboratory.

Lee, P. L., Shu, D., Ramanathan, M., Preissner, C., Wang, J., Beno, M. A., Von Dreele, R. B., Ribaud, L., Kurtz, C., Antao, S. M., Jiao, X., and Toby, B. H. (**2008**). "A twelve-analyzer detector system for high-resolution powder diffraction," J. Synchrotron Radiat. **15**(5), 427–432.

Macrae, C. F., Bruno, I. J., Chisholm, J. A., Edington, P. R., McCabe, P., Pidcock, E., Rodriguez-Monge, L., Taylor, R., van de Streek, J., and Wood, P. A. (**2008**). "Mercury CSD 2.0 – new features for the visualization and investigation of crystal structures," J. Appl. Crystallogr. **41**, 466–470.

McKinnon, J. J., Spackman, M. A., and Mitchell, A. S. (**2004**). "Novel tools for visualizing and exploring intermolecular interactions in molecular crystals," Acta Crystallogr., B **60**, 627–668.

MDI (**2014**). *Jade 9.5* (Materials Data. Inc., Livermore, CA).

O'Boyle, N., Banck, M., James, C. A., Morley, C., Vandermeersch, T., and Hutchison, G. R. (**2011**). "Open Babel: an open chemical toolbox," J. Chem. Inform. **3**, 33. Doi: 10.1186/1758-2946-3-33.

Overeem, A. and Vinent, H. T. (**2008**). "Polymorphs of rivastigmine hydrogentartrate," US Patent Application 2008/0255231.

Shields, G. P., Raithby, P. R., Allen, F. H., and Motherwell, W. S. (**2000**). "The assignment and validation of metal oxidation states in the Cambridge Structural Database," Acta Crystallogr. B: Struct. Sci. **56**(3), 455–465.

Spackman, M. A. and Jayatilaka, D. (**2009**). "Hirshfeld surface analysis," Cryst. Eng. Comm. **11**, 19–32.

Stephens, P. W. (**1999**). "Phenomenological model of anisotropic peak broadening in powder diffraction," J. Appl. Crystallogr. **32**, 281–289.

Sykes, R. A., McCabe, P., Allen, F. H., Battle, G. M., Bruno, I. J., and Wood, P. A. (**2011**). "New software for statistical analysis of Cambridge Structural Database data," J. Appl. Crystallogr. **44**, 882–886.

Thompson, P., Cox, D. E., and Hastings, J. B. (**1987**). "Rietveld refinement of Debye-Scherrer synchrotron X-ray data from Al_2O_3," J. Appl. Crystallogr. **20**(2), 79–83.

Toby, B. H. (**2001**). "EXPGUI, a graphical user interface for GSAS," J. Appl. Crystallogr. **34**, 210–213.

van de Streek, J. and Neumann, M. A. (**2014**). "Validation of molecular crystal structures from powder diffraction data with dispersion-corrected density functional theory (DFT-D)," Acta Crystallogr., B: Struct. Sci., Cryst. Eng. Mater., **70**(6), 1020–1032.

Wang, J., Toby, B. H., Lee, P. L., Ribaud, L., Antao, S. M., Kurtz, C., Ramanathan, M., Von Dreele, R. B., and Beno, M. A. (**2008**). "A dedicated powder diffraction beamline at the Advanced Photon Source: commissioning and early operational results," Rev. Sci. Instrum. **79**, 085105.

Wavefunction, Inc. (**2013**). Spartan '14 Version 1.1.0, Wavefunction Inc., 18401 Von Karman Ave., Suite 370, Irvine CA 92612.

Wolff, S. K., Grimwood, D. J., McKinnon, M. J., Turner, M. J., Jayatilaka, D., and Spackman, M. A. (**2012**). *CrystalExplorer Version 3.1* (University of Western Australia, Perth, Western Australia).